

Analogue of electromagnetically induced transparency in integrated plasmonics with radiative and subradiant resonators

Ting Wang, Yusheng Zhang, Zhi Hong and Zhanghua Han*

Centre for Terahertz Research, China Jiliang University, Hangzhou 310018, China

*zhanghua@outlook.com

Abstract: We propose the use of radiative and subradiant resonators coupled to a metal-insulator-metal waveguide to represent the three-level energy diagram in conventional atomic systems and demonstrate a new realization of on-chip plasmonic analogue of electromagnetically-induced transparency (EIT) in integrated plasmonics. The radiative resonator is achieved with the help of aperture-coupling while evanescent coupling is relied for the subradiant resonator. Numerical simulation results demonstrate well-pronounced intermediate transmission peak through the bus waveguide and also show that the EIT effect can be easily controlled by the relative position of the two Fabry-Perot resonators.

©2014 Optical Society of America

OCIS codes: (240.6680) Surface plasmons; (160.3918) Metamaterials.

References and links

1. K. J. Boller, A. Imamolu, and S. E. Harris, "Observation of electromagnetically induced transparency," *Phys. Rev. Lett.* **66**(20), 2593–2596 (1991).
2. Z. Li, Y. Ma, R. Huang, R. Singh, J. Gu, Z. Tian, J. Han, and W. Zhang, "Manipulating the plasmon-induced transparency in terahertz metamaterials," *Opt. Express* **19**(9), 8912–8919 (2011).
3. M. Fleischhauer, A. Imamoglu, and J. P. Marangos, "Electromagnetically induced transparency: Optics in coherent media," *Rev. Mod. Phys.* **77**(2), 633–673 (2005).
4. C. Liu, Z. Dutton, C. H. Behroozi, and L. V. Hau, "Observation of coherent optical information storage in an atomic medium using halted light pulses," *Nature* **409**(6819), 490–493 (2001).
5. N. Papasimakis, V. A. Fedotov, N. I. Zheludev, and S. L. Prosvirnin, "Metamaterial analog of electromagnetically induced transparency," *Phys. Rev. Lett.* **101**(25), 253903 (2008).
6. D. D. Smith, H. Chang, K. A. Fuller, A. Rosenberger, and R. W. Boyd, "Coupled-resonator-induced transparency," *Phys. Rev. A* **69**(6), 063804 (2004).
7. K. Totsuka, N. Kobayashi, and M. Tomita, "Slow light in coupled-resonator-induced transparency," *Phys. Rev. Lett.* **98**(21), 213904 (2007).
8. Z. Han and S. I. Bozhevolnyi, "Plasmon-induced transparency with detuned ultracompact Fabry-Perot resonators in integrated plasmonic devices," *Opt. Express* **19**(4), 3251–3257 (2011).
9. R. D. Kekatpure, E. S. Barnard, W. Cai, and M. L. Brongersma, "Phase-coupled plasmon-induced transparency," *Phys. Rev. Lett.* **104**(24), 243902 (2010).
10. S. Zhang, D. A. Genov, Y. Wang, M. Liu, and X. Zhang, "Plasmon-induced transparency in metamaterials," *Phys. Rev. Lett.* **101**(4), 047401 (2008).
11. R. Singh, C. Rockstuhl, F. Lederer, and W. Zhang, "Coupling between a dark and a bright eigenmode in a terahertz metamaterial," *Phys. Rev. B* **79**(8), 085111 (2009).
12. S. Y. Chiam, R. Singh, C. Rockstuhl, F. Lederer, W. Zhang, and A. A. Bettiol, "Analogue of electromagnetically induced transparency in a terahertz metamaterial," *Phys. Rev. B* **80**(15), 153103 (2009).
13. N. Liu, L. Langguth, T. Weiss, J. Kästel, M. Fleischhauer, T. Pfau, and H. Giessen, "Plasmonic analogue of electromagnetically induced transparency at the Drude damping limit," *Nat. Mater.* **8**(9), 758–762 (2009).
14. N. Liu, T. Weiss, M. Mesch, L. Langguth, U. Eigenthaler, M. Hirscher, C. Sönnichsen, and H. Giessen, "Planar metamaterial analogue of electromagnetically induced transparency for plasmonic sensing," *Nano Lett.* **10**(4), 1103–1107 (2010).
15. P. Tassin, L. Zhang, T. Koschny, E. N. Economou, and C. M. Soukoulis, "Low-loss metamaterials based on classical electromagnetically induced transparency," *Phys. Rev. Lett.* **102**(5), 053901 (2009).
16. J. Zhang, S. Xiao, C. Jeppesen, A. Kristensen, and N. A. Mortensen, "Electromagnetically induced transparency in metamaterials at near-infrared frequency," *Opt. Express* **18**(16), 17187–17192 (2010).

17. S. I. Bozhevolnyi, A. B. Evlyukhin, A. Pors, M. G. Nielsen, M. Willatzen, and O. Albrektsen, "Optical transparency by detuned electrical dipoles," *New J. Phys.* **13**(2), 023034 (2011).
18. Q. Xu, S. Sandhu, M. L. Povinelli, J. Shakya, S. Fan, and M. Lipson, "Experimental realization of an on-chip all-optical analogue to electromagnetically induced transparency," *Phys. Rev. Lett.* **96**(12), 123901 (2006).
19. Y. Zhang, S. Darmawan, L. Y. M. Tobing, T. Mei, and D. H. Zhang, "Coupled resonator-induced transparency in ring-bus-ring Mach-Zehnder interferometer," *J. Opt. Soc. Am. B* **28**(1), 28–36 (2011).
20. Z. Han, V. Van, W. N. Herman, and P. T. Ho, "Aperture-coupled MIM plasmonic ring resonators with sub-diffraction modal volumes," *Opt. Express* **17**(15), 12678–12684 (2009).

1. Introduction

Electromagnetically induced transparency (EIT) is a quantum interference phenomenon which can be observed in atomic systems when a strong external optical field is applied [1] to the medium. The sharp transparency window with narrow spectral width in the absorption band, accompanied with extraordinarily steep dispersion, is important to achieve a dramatic group-velocity reduction in the propagating light and to realize a variety of novel effects [2]. A great many interesting potential applications based on EIT have appeared in a wide range of fields, such as slow light, enhanced optical nonlinearities and optical information storage [3, 4]. However, the realization of EIT in atom systems needs extreme experimental conditions like cryogenic conditions and gaseous medium, restricting the practical applications of EIT. Recently, mimicking EIT in classical configurations has attracted tremendous attention and various schemes have been proposed and demonstrated to display the EIT-like spectral responses [5], e.g. coupled-resonator-induced transparency [6,7], plasmon-induced transparency (PIT) [8, 9], metamaterial-induced transparency [10–16]. Among those reported schemes, the PIT in integrated plasmonics is of special interest for high intensity photonic integration due to the possibility of realizing devices with ultra small footprint, thanks to the subwavelength confinement ability provided by plasmonic waveguides [8].

As we have pointed out in [8], the phenomenon of EIT can be considered using two alternative ways: as resulting from the destructive interference between two pathways involving the bare, dipole-allowed and metastable, states or, equivalently, the doublet of dressed states (created by the strong pump radiation) representing two closely spaced resonances decaying to the same continuum [1]. Figure 1 illustrates schematically the energy level diagrams of the two cases in atomic systems. In a typical three-level atomic system as shown in Fig. 1(a), dipole allowed transitions make both the ground state $|1\rangle$ and metastable state $|2\rangle$ coupled to the excited state $|3\rangle$ via the applied field while transition between $|1\rangle$ and $|2\rangle$ is forbidden. There are two different transition pathways $|1\rangle \rightarrow |3\rangle$ and $|1\rangle \rightarrow |3\rangle \rightarrow |2\rangle \rightarrow |3\rangle$ with which an atom in the ground state can experience the transition to the excited state. Equivalently, the excited state $|3\rangle$ shown as the dashed line in Fig. 1(b) will split into two dressed states $|\pm\rangle = (|3\rangle \pm |2\rangle) / \sqrt{2}$ when a strong electromagnetic field was applied. So the atoms in the ground state can be excited to either $|+\rangle$ or $|-\rangle$ [3]. Although these two physical pictures are equivalent to each other when dealing with the EIT phenomenon in atomic systems, their realization with classical systems depends on the EIT mechanism that is imitated [17]. The first picture suggests employing radiative and subradiant elements that are mutually coupled. Alternatively viewed, the EIT is achieved due to the cancellation of opposite contributions from two detuned resonances, which are equally spaced but with opposite signs of detuning from the probe frequency. In metamaterial-induced transparency, examples of the first picture can be found as metamaterials with the unit cell composed of bright and dark elements [10, 11, 14, 16] which have been widely investigated in recent years in different regions of the electromagnetic spectrum. Detuned dipoles [17] appear recently as the realization of metamaterial-induced transparency following the second

picture. In coupled-resonator-induced transparency with dielectric waveguides one can find cascaded ring resonators on the **same side** of the bus waveguide [6] as the representative for the first case and **detuned ring resonators** [18, 19] for the second. In integrated plasmonics circuit which has the potential to realize ultra compact devices, detuned resonators [8, 9] have been investigated to realize PIT representing the second picture in Fig. 1, however, it is rarely reported to use the first picture to achieve the same functionality.

In this paper we propose to use mutually coupled radiative and subradiant resonators representing the three-level energy diagram atomic systems to realize the analogue of EIT in integrated plasmonics. Both the bus waveguide and the resonators are in the form of metal-insulator-metal (MIM) waveguides. An aperture between the bus waveguide and the radiative resonator is used to provide the high coupling, as is also required between the bright element and free space in metamaterial-induced transparency. Evanescent coupling is relied between the radiative and subradiant resonators. Numerical results show that well-pronounced EIT-like transmission can be demonstrated with this structure, and the transmission height can be controlled by changing the coupling strength between the two resonators when the aperture dimension is kept unchanged.

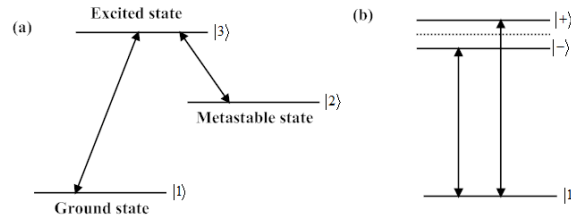


Fig. 1. Energy level diagrams in atomic systems when EIT can be observed. (a) A three-level atomic system where the transition between the continuum and the metastable state is prohibited; (b). The doublet of dressed states equivalent to (a) when a strong optical field is applied to the transition between the excited state and metastable state.

2. Radiative and subradiant resonators in MIM waveguides

Unlike the case when two detuned aperture-coupled Fabry-Perot (FP) resonators are placed on the opposite side of the bus waveguide [8], which is shown in Fig. 2(a) and corresponds to two dressed states in Fig. 1(b), we use two Fabry-Perot resonators on the same side of the bus waveguide to represent the picture of Fig. 1(a). Figure 2(b) illustrates the geometry of the structure investigated in this paper. Both the bus waveguide and the two resonators are in the form of MIM waveguide with the same cross section, which is composed of a thin SiO_2 layer embedded in the Ag background. The permittivity of Ag is described by the Drude model $\epsilon_{Ag} = \epsilon_{\infty} - \omega_p^2 / (\omega^2 + j\gamma\omega)$, where ϵ_{∞} represents the permittivity at infinite angular frequency and is chosen as 3.7, ω_p is the bulk plasma frequency with the value of 9.1eV and γ is the oscillation damping of electrons and the value is 0.018eV [8]. The width of SiO_2 is 100nm and its index is assumed to be 1.45. The two resonators are separated by a distance t . The first (1st) resonator with length L_1 is side-coupled to the bus waveguide with an aperture whose width d is constantly kept as 50nm throughout this paper. The aperture will ensure a strong coupling between the resonator and the bus waveguide [20], making the resonator behave as a radiative resonator like the bright element in metamaterial-induced transparency. The gap between the 1st resonator and the bus waveguide is 50nm, fully realizable with current nanofabrication techniques. The second (2nd) resonator with length L_2 is evanescently coupled to the 1st resonator, with a weaker coupling than that between the 1st resonator and the bus waveguide. Since the metal walls are optically thick and the 2nd resonator can only be coupled to the bus waveguide via the first resonator, it works as the “dark” subradiant

resonator. The bus waveguide, the 1st resonator and the 2nd resonator serve as the ground state $|1\rangle$, the excited state $|3\rangle$ and the metastable state $|2\rangle$ shown in Fig. 1(a) respectively.

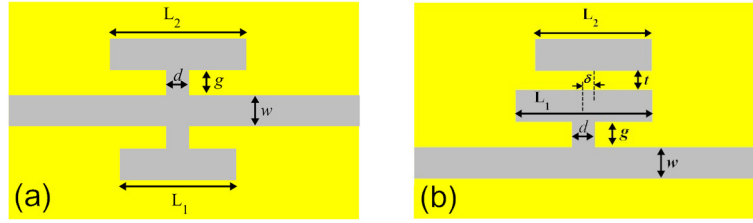


Fig. 2. Schematics of the structures (a) two aperture-coupled FP resonators are placed on the opposite side of the bus waveguide representing the dressed states in Fig. 1(b); (b) two resonators are on the same side of the waveguide representing the three-level diagram in Fig. 1(a).

The eigen plasmonic mode of the bus waveguide is used from the left port to excite the structure and the transmission is calculated using the power arriving at the exit port normalized to the incident power. The finite element method is used for the numerical simulations and by scanning the wavelength of the incident light, the transmission spectrum can be obtained.

3. Results and discussion

First we give the result when the centers of the two resonators match each other along the propagation direction of the bus waveguide, i.e. the lateral shift δ shown in Fig. 2(b) equals to 0. In all the simulations L_1 is set to be 600nm while L_2 is 550nm giving rise to the excitation of the 2nd order FP resonator mode whose magnetic field is symmetric along the central plane of FP resonators. Note that the 1st resonator is 50nm longer than the 2nd one to have the same resonant wavelength due to a negative role that the aperture plays in the overall optical path of the resonator. The black line in Fig. 3(a) shows the transmission spectrum when the distance t between the two resonators is 50nm and one can see a well-pronounced intermediate transmission peak with the value as high as 0.74 at the wavelength of 1035nm between two transmission dips, demonstrating a well-known feature of the EIT-like effect. The distribution of the magnetic field are presented in Figs. 3(b)-3(d) for the wavelengths of the two transmission dips ($\lambda_1 = 1023\text{nm}$ and $\lambda_2 = 1053\text{nm}$) and the transmission peak ($\lambda_3 = 1035\text{nm}$). It is quite distinct that at the two transmission dips both the two resonators are strongly excited. However at 1023nm the magnetic fields in the two resonators are in-phase while at 1053nm they are out-of-phase. Notably, at the transmission peak only one FP resonator is excited while the field in the other resonator is much weaker. This phenomenon is quite different with that demonstrated in plasmon-induced transparency with detuned resonators [8], where at the two transmission dips only one resonator is excited while at the transmission peak both resonators are excited with the phase opposite. As we mentioned before, the phenomenon of EIT in atomic systems can be considered using two alternative but equivalent ways shown in Fig. 1. In a similar way we can explain the magnetic field distribution shown in Fig. 3. Although the geometry represents the diagram shown in Fig. 1(a), the mutual coupling between the two FP resonators will result in a splitting of the original resonance into two super resonances like the picture shown in Fig. 1(b). Each dip in the transmission spectrum corresponds to a super resonance. Since the splitting of the original resonance is correlated with the coupling, the difference in the wavelength between the two transmission dips is a sign of the coupling strength between the two resonators. Similar to the two super waveguide modes when two straight waveguides are placed in parallel and coupled to each other, at one super resonance the fields at the two resonators are in-phase while at the other they are out-of-phase, as shown in Figs. 3(b) and 3(d). At the transmission peak both the

super resonances are excited so that the field in one resonator is cancelled while that in the other resonator is enhanced. Different optical pathways from the bus waveguide to the two super resonances will experience a destructive interference, which cancels the original resonance effect at the transmission peak and lead to the formation of the EIT effect observed.

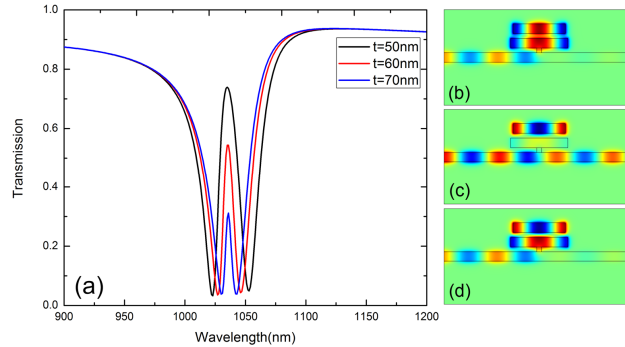


Fig. 3. (a) Simulated EIT-like transmission spectra for two resonators with $L_1 = 600\text{nm}$, $L_2 = 550\text{nm}$, (b) ~ (d) Distribution of the real part of the magnetic field at resonance wavelengths of 1023nm, 1035nm and 1053nm when t equals to 50nm.

From the theory of EIT in atomic systems one knows that the EIT effect is related with the Rabi frequency of the control field (the frequency between $|+\rangle$ and $|-\rangle$), which reflects the coupling between the excited state and the metastable state shown in Fig. 1(a). Since the two states are represented by the two FP resonators in our proposal, one can easily control the EIT phenomenon by adjusting coupling strength between the two resonators. The easiest way is to vary the distance t between the two to control the field from one resonator penetrating the metal wall into the other. Figure 3(a) presents the transmission spectra when t is increased from 50nm to 70nm with a step of 10nm. The transmission at peak drops from 0.74 to 0.54 and 0.31, and the wavelength difference between the two transmission dips is also changed from 30nm to 19nm and 13nm. These results clearly show that increasing t will result in a lower value of the transmission peak at the same wavelength, along with a smaller wavelength difference in the two transmission dips, which demonstrates a smaller resonance splitting due to a weaker coupling between the two resonators.

It is quite straightforward to change t to control the coupling between the two resonators. Unlike the ring resonators, the FP resonators support only standing waves at resonances, one can alternatively manipulate the overlap between the fields in the two resonators by shifting the relative position of the standing wave patterns, and then the coupling can also be changed at resonant wavelengths. If the node of the standing wave in one resonator matches spatially the antinode of the other resonator, the coupling will be the minimum. As an example, the distance t between the two resonators is kept as 60nm now while the center of the 2nd resonator is shifted by a lateral displacement δ compared to that of the 1st resonator, which is schematically shown in Fig. 2(b). Figure 4(a) shows the transmission spectra when the shift δ is changed from 0nm to 50nm and 100nm. It's evidently shown that as δ increases the transmission peak drops and the wavelength difference between the two transmission dips also becomes smaller, demonstrating that the coupling between the resonators is weaker. Figures 4(b)-4(d) give the magnetic field distribution of the transmission dips and peak when δ equals to 50nm, quite similar to the field shown in Fig. 3. The shift of the relative position between the centers of the two FP resonators provides a new means of controlling the coupling strength.

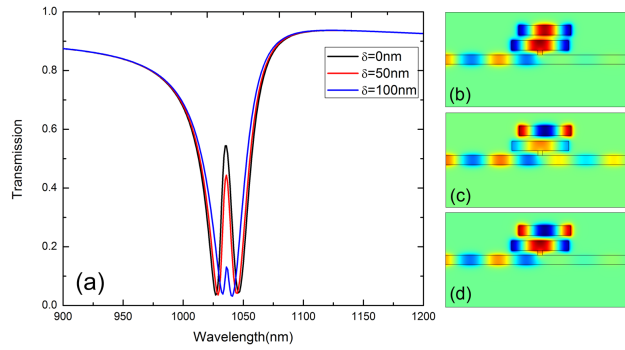


Fig. 4. EIT-like transmission spectra (a) for different lateral displacement δ calculated at $t = 60\text{nm}$; (b) ~ (d) Distribution of the real part of the magnetic field at resonance wavelengths of 1029nm, 1036nm and 1045nm with $\delta = 50\text{nm}$.

4. Summary

In conclusion, a new scheme consisting of radiative and subradiant resonators in MIM waveguide is proposed to mimic the three-level energy diagram in atomic systems and the EIT-like spectral response in near infrared in integrated plasmonics is numerically demonstrated with this scheme. The mutual coupling of two resonators gives rise to the splitting of the original resonance into two super resonances. Different optical pathways between the bus waveguide and the two super resonances result in a transparency peak in the absorption window. The EIT-like behavior can be well engineered by changing the relative position between the radiative and subradiant resonators to tune the coupling strength between the two. This proposed new scheme represents a great supplement to the analogue of EIT in integrated plasmonics using detuned resonators and we expect that some novel functionality can be further introduced into guided plasmonic circuits.

Acknowledgments

This work was supported by the National Natural Science Foundation of China (61107042).